Article

Developmental Cell

A Conserved Role for Girdin in Basal Body Positioning and Ciliogenesis

Highlights

- Girdin regulates cilia morphology in *C. elegans* sensory neurons and RPE-1 cells
- Girdin localizes to the proximal regions of centrioles in ciliated cells
- Basal body positioning is disrupted upon Girdin knockdown
- Girdin is required to localize rootletin at basal bodies

Authors

Inna V. Nechipurenko, Anique Olivier-Mason, Anna Kazatskaya, ..., Maxwell G. Heiman, Oliver E. Blacque, Piali Sengupta

Correspondence

ivn@brandeis.edu (I.V.N.), sengupta@brandeis.edu (P.S.)

In Brief

The mechanisms by which basal bodies are positioned to template ciliogenesis at the correct cellular location are largely unknown. Nechipurenko et al. show that the signaling and scaffolding protein Girdin regulates basal body positioning and ciliogenesis, in part via localization of rootletin in *C. elegans* sensory neurons and human cells.

Nechipurenko et al., 2016, Developmental Cell *38*, 493–506
September 12, 2016
http://dx.doi.org/10.1016/j.devcel.2016.07.013

CellPress

Developmental Cell
Article

A Conserved Role for Girdin in Basal Body Positioning and Ciliogenesis

Inna V. Nechipurenko,[1,*] Anique Olivier-Mason,[1] Anna Kazatskaya,[1] Julie Kennedy,[2] Ian G. McLachlan,[3] Maxwell G. Heiman,[3] Oliver E. Blacque,[2] and Piali Sengupta[1,4,*]
[1]Department of Biology and National Center for Behavioral Genomics, Brandeis University, Waltham, MA 02454, USA
[2]School of Biomolecular and Biomedical Science, University College Dublin, Belfield, Dublin 4, Ireland
[3]Department of Genetics, Harvard Medical School and Boston Children's Hospital, Boston, MA 02115, USA
[4]Lead Contact
*Correspondence: ivn@brandeis.edu (I.V.N.), sengupta@brandeis.edu (P.S.)
http://dx.doi.org/10.1016/j.devcel.2016.07.013

SUMMARY

Primary cilia are ubiquitous sensory organelles that mediate diverse signaling pathways. Cilia position on the cell surface is determined by the location of the basal body (BB) that templates the cilium. The mechanisms that regulate BB positioning in the context of ciliogenesis are largely unknown. Here we show that the conserved signaling and scaffolding protein Girdin localizes to the proximal regions of centrioles and regulates BB positioning and ciliogenesis in *Caenorhabditis elegans* sensory neurons and human RPE-1 cells. Girdin depletion alters localization of the intercentriolar linker and ciliary rootlet component rootletin, and rootletin knockdown in RPE-1 cells mimics Girdin-dependent phenotypes. *C. elegans* Girdin also regulates localization of the apical junction component AJM-1, suggesting that in nematodes Girdin may position BBs via rootletin- and AJM-1-dependent anchoring to the cytoskeleton and plasma membrane, respectively. Together, our results describe a conserved role for Girdin in BB positioning and ciliogenesis.

INTRODUCTION

Primary cilia are microtubule (MT)-based sensory organelles that are present on diverse cell types in metazoans. Cilia play critical signaling roles, and ciliary dysfunction underlies a range of human syndromes termed ciliopathies (Brown and Witman, 2014; Lancaster and Gleeson, 2009). Ciliary structure and mechanisms of ciliogenesis are remarkably conserved, highlighting the importance of these organelles in animal development and cellular homeostasis. However, despite our increased knowledge about this organelle in recent years, much remains to be understood about how cilia are built and how they function.

Cilia in all organisms are nucleated by the basal body (BB) derived from the mother centriole. Ciliogenesis is generally initiated as BBs migrate toward, and dock at, the cell surface. Subsequently, the transition zone (TZ) that gates ciliary protein trafficking is templated, and intraflagellar transport (IFT) components are recruited to elongate the ciliary axoneme (Dawe et al., 2007; Reiter et al., 2012). Thus, final intracellular BB position determines the cell surface location of the cilium. For example, in non-polarized cells, the BB and cilium are positioned near the cell center in close proximity to the nucleus, whereas in migrating cells BBs and cilia are positioned ahead of the nucleus in the leading process (Elric and Etienne-Manneville, 2014; Tang and Marshall, 2012). The mechanisms underlying directional migration and positioning of BBs are poorly understood.

Caenorhabditis elegans provides a compelling model system in which to explore the regulatory pathways of BB positioning and ciliogenesis. *C. elegans* has 60 ciliated cells, all of which are sensory neurons; 12 and two pairs of these neurons are found in the bilateral amphid and phasmid organs in the head and tail, respectively, and possess cilia at their dendritic tips (Doroquez et al., 2014; Perkins et al., 1986; Ward et al., 1975). Live imaging of *C. elegans* embryos has shown that amphid sensory dendrites elongate from the soma via retrograde extension, such that the emerging dendrite is anchored at the presumptive nose, while the cell body translocates posteriorly (Heiman and Shaham, 2009; Sulston et al., 1983). BBs are localized to the dendritic tips, thus ensuring cilia formation at this location. Unlike in mammals, BBs in *C. elegans* are thought to degenerate or remodel following initiation of ciliogenesis in embryos (Dammermann et al., 2009; Perkins et al., 1986). However, early steps of ciliogenesis have not been visualized in *C. elegans*, and the mechanisms regulating BB positioning in sensory neurons remain uncharacterized in this organism.

Here we show that the signaling and scaffolding protein Girdin is required to position BBs and regulate ciliogenesis in *C. elegans* sensory neurons and human RPE-1 cells. We find that Girdin is localized to the proximal regions of centrioles and regulates centriolar localization of rootletin, a component of the intercentriolar tether and ciliary rootlets. Decreased rootletin function in RPE-1 cells results in phenotypes similar to those observed upon Girdin knockdown, suggesting that rootletin-mediated anchoring of the BBs to the cytoskeleton may underlie BB positioning defects upon reduction of Girdin function. Girdin-dependent localization of the apical junction component AJM-1 at sensory neuron dendritic tips may also contribute to BB anchoring and cilia formation in *C. elegans*. Together, our results define Girdin as a critical and conserved regulator of BB positioning and ciliogenesis in nematodes and human cells.

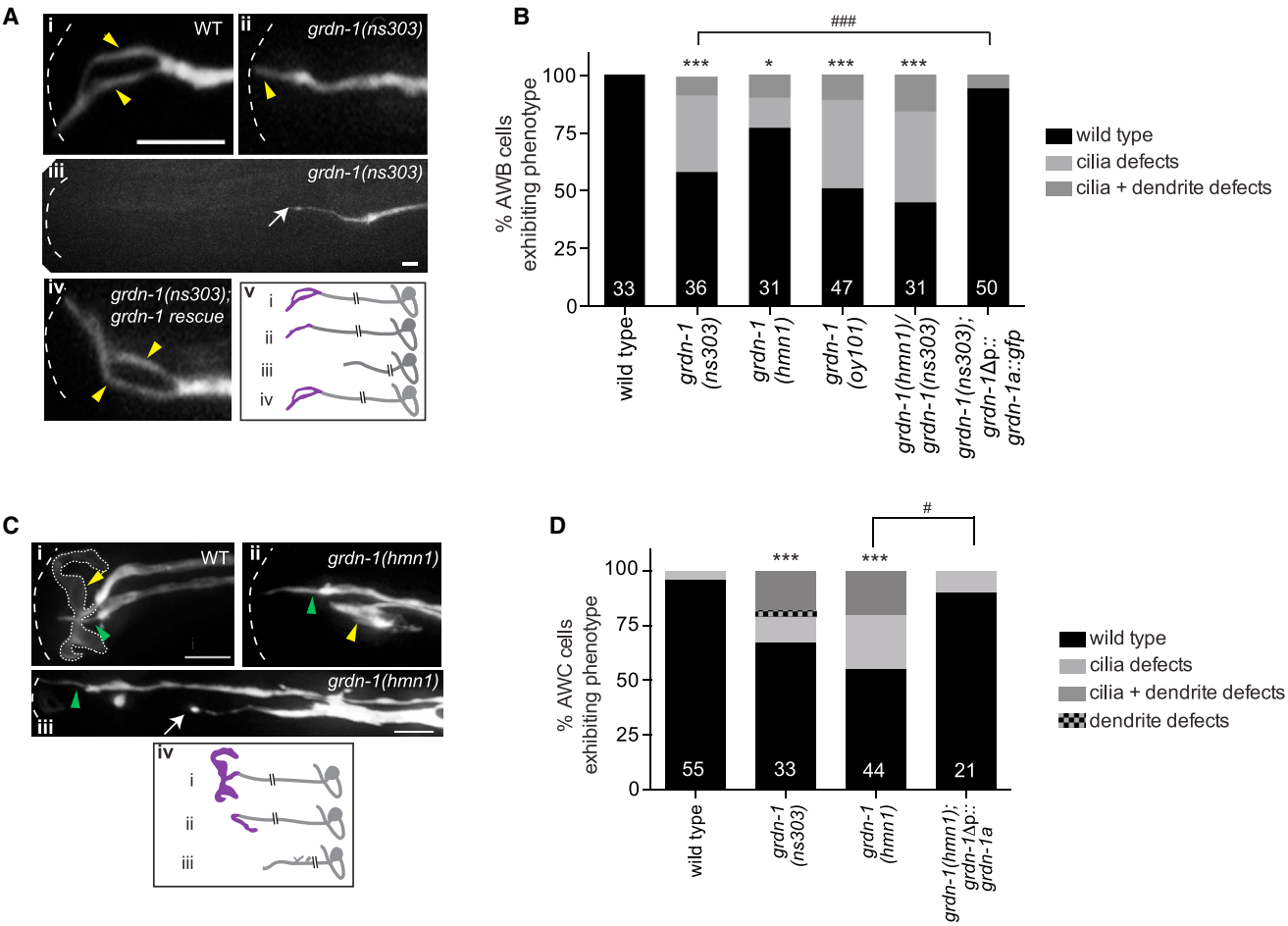

Figure 1. *C. elegans* GRDN-1 Regulates Ciliogenesis in Multiple Sensory Neuron Types

(A) (Ai–Aiv) Images of AWB cilia and (Av) cartoons of AWB neurons in the indicated genetic backgrounds. Cilia are marked by yellow arrowheads (Ai–Aiv) or drawn in purple (Av). White arrow indicates a truncated dendrite (Aiii). Neuronal morphology was visualized via *str-1*p::*gfp* expression. Scale bars represent 5 μm in (Ai) and 2 μm in (Aiii). White dashed lines mark the worm nose. Anterior is to the left.

(B) Quantification of morphological defects in AWB neurons in the shown genetic backgrounds. Number of cells examined per genotype is indicated. Cilia defects include loss of one or both cilia and morphologically aberrant cilia. Dendritic defects include variably shortened processes with aberrant or no ciliary structures. *$p < 0.05$ and ***$p < 0.001$, different from wild-type; $^{\#\#\#}p < 0.001$, different between indicated values (chi-square test).

(C) (Ci–Ciii) Images of AWC cilia and (Civ) cartoons of AWC neurons in the indicated genetic backgrounds. Cilia are marked by yellow arrowheads (Ci, Cii) or drawn in purple (Civ). Green arrowheads mark ASE cilia. The wild-type AWC cilium is outlined by a dotted white line in (Ci). White arrow indicates a shortened dendrite (iii). Neuronal morphologies were visualized via expression of *ceh-36*p::*gfp* in AWC and ASE. Scale bars represent 5 μm in (Ci) and 2 μm in (Ciii). White dashed lines mark the worm nose. Anterior is to the left.

(D) Quantification of morphological defects in AWC neurons in the shown genetic backgrounds. Number of cells examined per genotype is indicated. Cilia defects include loss, or reduction, of the membranous fans. Dendritic defects include shortened processes with or without a cilium, or branched dendrites. ***$p < 0.001$, different from wild-type; $^{\#}p < 0.05$, different between indicated values (chi-square test).

See also Figure S1 and Table S1.

RESULTS

Girdin Regulates Cilia Morphology in Multiple Sensory Neuron Types in *C. elegans*

In a candidate screen for mutants with sensory cilia defects, we identified the *oy101* allele as a background mutation in the RB771 strain. Subsequent analyses indicated that *oy101* was allelic to the *ns303* and *hmn1* alleles; all three mutations affect the *grdn-1* locus (*Y51A2D.15*). One of the two cilia of AWB amphid sensory neurons was absent in a subset of *grdn-1* mutants (Figures 1A and 1B). As in wild-type, AWB cilia in *grdn-1* mutants contained the OSM-3 homodimeric kinesin-2 motor (Figure S1A), and this protein underwent IFT (Figure S1B), suggesting that axonemes are present in *grdn-1* cilia. In addition, a small but significant fraction of AWB dendrites was shortened to different extents in *grdn-1* animals (Figures 1A and 1B). All morphological defects were incompletely penetrant in all *grdn-1* alleles (Figure 1B). Thus, GRDN-1 regulates AWB neuronal morphology.

We next asked whether mutations in *grdn-1* affect cilia morphology of additional sensory neurons. Six neuron pairs, including the AWB neurons, in the amphid organs take up lipophilic dyes such as DiI (Perkins et al., 1986). *grdn-1* mutants

exhibited a partial dye-filling phenotype (Figure S1C), similar to that in mutants with cilia or dendritic defects in multiple neurons (Perkins et al., 1986; Starich et al., 1995). We confirmed that the morphologically complex cilia of the AWA and AWC sensory neurons, as well as the simpler, rod-like cilia of the ADL and ASI sensory neurons, exhibit partially penetrant defects in *grdn-1* alleles (Figures 1C, 1D, and S1D–S1F; Table S1). Similar to observations in AWB, dendritic morphologies of these neurons were also affected in a fraction of *grdn-1* mutants (Figures 1C, 1D, and S1D–S1F; Table S1). The processes of amphid sheath glia that are in close contact with sensory neurons and that contribute to shaping neuronal morphology (Bacaj et al., 2008; Doroquez et al., 2014; Ward et al., 1975; Ware et al., 1975) were grossly normal in *grdn-1* mutants (Figure S1G and Table S1). Taken together, these results indicate that GRDN-1 regulates ciliogenesis in multiple sensory neuron types.

grdn-1 Encodes the *C. elegans* Ortholog of Girdin

Genetic mapping followed by whole-genome resequencing and complementation showed that *oy101*, *ns303*, and *hmn1* are alleles of *grdn-1*. All three alleles failed to complement each other for the dye-filling defect (data not shown), and this defect was rescued by a GFP-tagged full-length *grdn-1* cDNA expressed under its endogenous promoter (Figure S1C). In addition, the AWB and AWC cilia defects were rescued upon expression of the *grdn-1* cDNA under *grdn-1* regulatory sequences (Figures 1A, 1B, and 1D).

grdn-1 encodes the *C. elegans* ortholog of mammalian Girdin, a signaling and scaffolding protein implicated in the regulation of diverse cellular processes including cell migration, cell division, autophagy, neurogenesis, and cancer cell metastasis (Enomoto et al., 2006; Garcia-Marcos et al., 2015; Weng et al., 2010). Recently, Girdin has also been implicated in dendritic morphogenesis in *Drosophila* sensory neurons (Ha et al., 2015). Similar to mammalian Girdin, *C. elegans* GRDN-1 contains a predicted MT-binding Hook domain at the N terminus, a central coiled-coil motif, and a Gα binding site (Figure 2A). However, the C terminus of GRDN-1 is divergent and lacks an obvious actin-binding or SH2 domain found in mammalian Girdin. Additionally, a GEF motif present in mammalian Girdin is not fully conserved in GRDN-1 (Coleman et al., 2016). Instead, the C terminus of GRDN-1 contains a GCV motif, which is present in the Girdin paralog Daple and interacts with Disheveled (Enomoto et al., 2006; Oshita et al., 2003) (Figure 2A).

The *grdn-1* locus in *C. elegans* is predicted to encode three protein isoforms. Unlike the a isoform, the b and c isoforms lack the GCV motif and Hook domains, respectively (Figure 2A). The causative lesion in the *oy101* allele is a 7-kb deletion located 3 kb upstream of the *grdn-1* translation start site. The *ns303* mutation is an early termination codon predicted to produce only the c isoform of GRDN-1, whereas the *hmn1* allele is a termination codon in the Gα binding motif predicted to encode truncated GRDN-1a, b, and c isoforms (Figure 2A). Thus, these alleles are unlikely to be null. Indeed, *grdn-1* appears to be an essential gene, since a *grdn-1*(*tm6493*) deletion allele (National BioResource Project, Japan) (Figures S2A and S2B) and RNAi-mediated *grdn-1* knockdown result in embryonic lethality with rare severely deformed L1 escaper larvae (I.V.N. and P.S., unpublished data), precluding analysis of cilia morphology. Thus, isolation of *grdn-1* hypomorphic alleles allowed us to uncover a role for this gene in ciliogenesis.

GRDN-1 Localizes to Basal Bodies in Sensory Neurons

To determine the expression pattern and subcellular localization of GRDN-1, we expressed a functional (Figure 2E) *gfp*-tagged *grdn-1a* cDNA construct under *grdn-1* regulatory sequences in the putative null *grdn-1*(*tm6493*) background. GRDN-1a::GFP was broadly expressed during embryogenesis and was enriched at the presumptive nose starting at mid-embryogenesis (Figure 2B), coinciding with the time period of sensory neuron differentiation and ciliogenesis (Sulston et al., 1983).

The subcellular localization of GRDN-1a::GFP was reminiscent of that previously reported for BB and TZ proteins in embryonic head sensory neurons (e.g., Dammermann et al., 2009). Consistent with this notion, GRDN-1a::GFP was present at the AWB cilia base in larvae (Figure 2B), and co-localized with the BB markers DYF-19 and GASR-8 in the PHA/PHB ciliated tail neurons in L1 larvae and adult AWB neurons, respectively (Figure 2C). Intriguingly, GRDN-1a::GFP appeared to be enriched at the proximal ends of centrioles, and was completely excluded from the TZ marked by MKS-5::tagRFP (Figure 2C). Together, these observations suggest that Girdin is localized to the BBs in *C. elegans* sensory neurons.

To characterize the GRDN-1 domains necessary for its localization to the BB region and function in ciliogenesis, we generated GFP-tagged GRDN-1 constructs lacking the predicted Hook domain (GRDN-1(ΔHook)), Gα binding motif (GRDN-1(ΔGα)), or part of the divergent C terminus including the GCV sequence (GRDN-1(ΔCt)) (Figure 2A). Since Girdin is regulated via phosphorylation by the Akt Ser/Thr kinase in some contexts (Enomoto et al., 2005), we also mutated a serine predicted to be phosphorylated by Akt to alanine (GRDN-1(S1095A)) (Figure 2A). Expression of mutant constructs in *grdn-1*(*tm6493*) animals under *grdn-1* regulatory sequences fully or partially rescued embryonic lethality (data not shown), allowing us to examine the effects of these mutations on cilia morphogenesis. All mutant GFP-tagged GRDN-1 proteins except for GRDN-1(ΔCt)::GFP localized normally to the AWB cilia base (Figure 2D). However, GRDN-1(ΔCt)::GFP was absent or mislocalized within AWB distal dendrites in >40% of examined *grdn-1*(*tm6493*) animals (Figure 2D). Consistent with these localization patterns, ~30% of *grdn-1*(*tm6493*) mutants expressing the GRDN1(ΔCt) but not full-length or other mutant fusion proteins exhibited AWB ciliary defects (Figure 2E). These results indicate that the C-terminal domain of GRDN-1 is necessary for its correct subcellular localization and function in ciliogenesis.

GRDN-1 Acts in Neurons during Early Development to Regulate Cilia Morphology

The majority of ciliated amphid sensory neurons are born between 250 and 450 min of embryogenesis (Sulston et al., 1983) and cilia are visible by the three-fold stage of embryonic development. Heat-shock-mediated induction of *grdn-1* expression at or before the comma stage of embryogenesis (<430 min) but not at later stages significantly rescued AWB defects in L4 or young adult animals (Figure 2F). Importantly, AWB cilia were unaffected upon heat-shocking wild-type animals during late embryogenesis (Figure 2F), indicating that the failure to rescue upon induction of

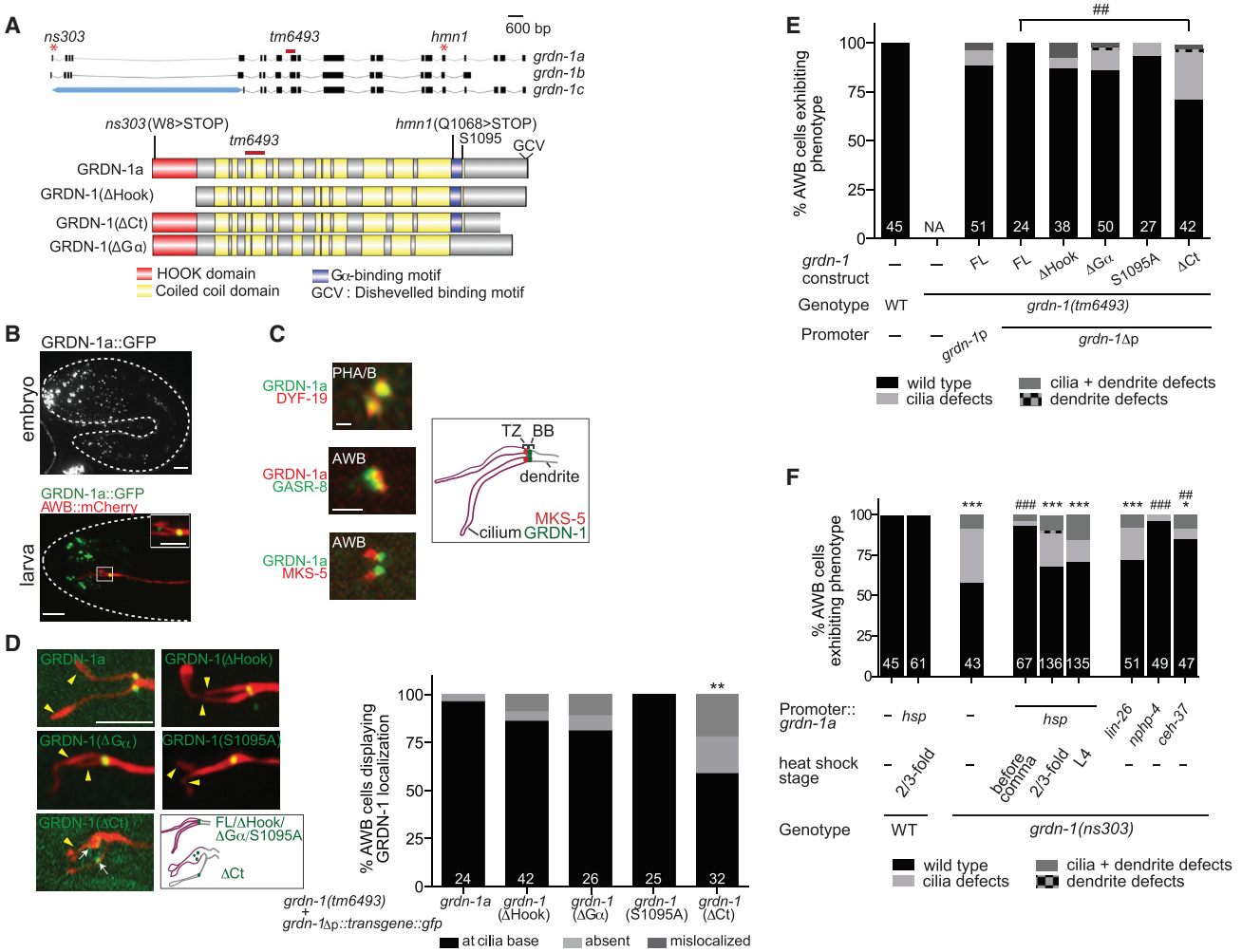

Figure 2. The *C. elegans* GRDN-1 Protein Is Expressed Embryonically and Localizes to BBs

(A) (Top) Gene structure of the predicted *grdn-1* isoforms. Filled black boxes represent exons. Blue box in *grdn-1c* represents the 5′ UTR. Red asterisks mark predicted termination codons in *grdn-1*(*ns303*) and *grdn-1*(*hmn1*) alleles. Red line marks the deletion in *grdn-1*(*tm6493*). (Bottom) Predicted domain organization of GRDN-1 and mutant proteins.

(B) Images of GRDN-1a::GFP driven under endogenous *grdn-1* regulatory sequences in a *grdn-1*(*tm6493*) 1.5-fold stage embryo (top) and a larva (bottom). The AWB cilia base is enlarged in the inset. Scale bar, 5 μm; scale bar in inset, 1 μm. White dashed lines outline the embryo and larva in the corresponding panels. Anterior is to the left.

(C) Images (left) and cartoon (right) showing localization of fusion proteins in PHA/PHB or AWB in wild-type L1 larvae or young adults, respectively. GRDN-1a::GFP was driven under its endogenous regulatory sequences (*grdn-1*p: PHA/PHB) or *str-1* promoter (AWB). GFP::GASR-8 and MKS-5::tagRFP were expressed under the *srd-23* and *str-1* promoters, respectively; DYF-19::tagRFP was expressed under *bbs-8* regulatory sequences. Scale bar, 1 μm.

(D) Images (left) and quantification (right) of localization patterns of GFP-tagged mutant GRDN-1 proteins expressed under 1.7 kb of *grdn-1* regulatory sequences (*grdn-1*Δp) in *grdn-1*(*tm6493*) animals. AWB was visualized via *str-1*p::mCherry expression. Yellow arrowheads mark the AWB cilia; white arrows mark mislocalized GRDN-1 constructs. Number of cells per genotype is indicated. **p < 0.01, different from *grdn-1*(*tm6493*) expressing the full-length GRDN-1a fusion protein (Fisher's exact test). Scale bar, 5 μm. Anterior is to the left.

(E) Quantification of AWB morphological phenotypes in wild-type (WT) or *grdn-1*(*tm6493*) animals expressing the indicated *gfp*-tagged *grdn-1* constructs under *grdn-1*Δp or *grdn-1*p sequences. ##p < 0.01, different between indicated values (Fisher's exact test). FL, full-length.

(F) Quantification of AWB morphological defects in wild-type or *grdn-1*(*ns303*) animals expressing the indicated transgenes with or without heat-shock treatment. AWB cilia of adult animals were visualized via *str-1*p::*gfp* expression. Number of cells scored per genotype is indicated. WT data are repeated from (E). *p < 0.05 and ***p < 0.001, different from wild-type; ##p < 0.01 and ###p < 0.001, different from *grdn-1*(*ns303*) (chi-square test).

See also Figure S2.

grdn-1 expression at later stages was not due to heat-induced defects in AWB cilia structure. Thus, *grdn-1* is required during or shortly after AWB formation to regulate ciliogenesis.

We next investigated the spatial requirement for *grdn-1* function in the regulation of sensory neuron morphology. Expression of *grdn-1a* under the ciliated neuron-specific *nphp-4* but not the glia-specific *lin-26* promoters rescued AWB defects in *grdn-1*(*ns303*) mutants (Figure 2F), suggesting that GRDN-1 acts in neurons to regulate ciliogenesis. Moreover, conditional mutants generated via CRISPR-Cas9 gene editing induced in ciliated

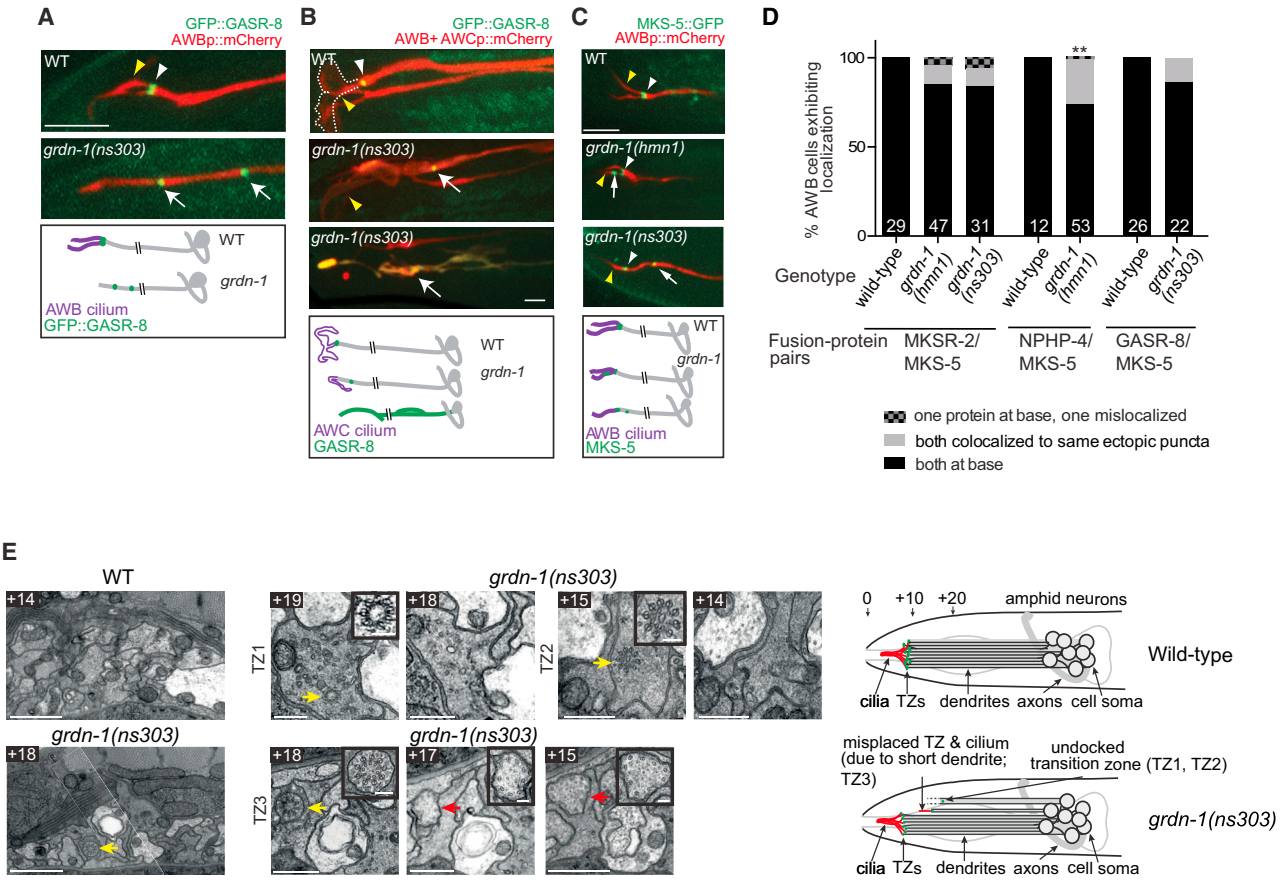

Figure 3. GRDN-1 Regulates Localization of a Subset of TZ and BB Proteins in *C. elegans* Sensory Neurons

(A–C) Images (top panels) and cartoons (bottom panels) of GFP::GASR-8 (A and B) and MKS-5::GFP (C) localization in AWB or AWC neurons in wild-type (WT) and *grdn-1* animals. Cilia are marked by yellow arrowheads in images and drawn in purple in cartoons. White arrowheads indicate the cilia base; ectopic localization is indicated by white arrows. The AWC cilium is outlined in white in (B). Scale bar, 5 μm. Anterior is to the left. See Table 1 for quantification.

(D) Quantification of co-localization of indicated fusion protein pairs in wild-type and *grdn-1* mutant AWB neurons. Only neurons in which expression of both fusion proteins was observed are included. Number of examined neurons is indicated. **$p < 0.01$, different from fusion protein co-localization predicted by chance (chi-square test).

(E) Low- and high-magnification (insets) TEM images, captured from serial cross-sections of the amphid pore region of wild-type (WT) and *grdn-1*(*ns303*) animals. Boxed numbers refer to the position of the imaged section relative to the distal-most first section ("0") at the pore opening (section position numbers are also indicated in schematic at right). In *grdn-1* mutants, TZ1 and TZ2 are misplaced distally, are undocked from the dendritic plasma membrane (yellow arrows in +19 and +15 images), and fail to extend a cilium (images +18 and +14). The dendrites of these neurons continue to extend anteriorly toward the nose tip (black hashed lines in bottom schematic at right). TZ3 is docked normally at the dendritic plasma membrane (yellow arrow in +18 image), and extends a cilium at the distal dendrite ending (red arrows in +17 and +15 images); thus, TZ3 is misplaced due to dendritic truncation. Scale bars represent 100 nm in high-magnification images, and 1 μm and 500 nm in low-magnification images of WT and *grdn-1* mutants, respectively.

See also Figures S3 and S4.

neurons (Shen et al., 2014) exhibited AWB defects (Figure S2C). Finally, AWB defects in *grdn-1*(*ns303*) animals were significantly rescued upon expression of *grdn-1* under the *ceh-37* promoter (Figure 2F) that drives expression transiently, but not exclusively, in the AWB neurons shortly after their birth (Lanjuin et al., 2003; Walton et al., 2015). These results suggest, but do not confirm, that *grdn-1* acts cell-autonomously during early embryogenesis to regulate AWB morphology.

GRDN-1 Regulates Localization of Basal Body and Transition Zone Components in *C. elegans* Cilia

To explore the mechanisms of GRDN-1-regulated ciliogenesis, we examined the subcellular localization of ciliary components in *grdn-1* mutants. Since GRDN-1 co-localizes with BBs, we first examined whether BB proteins are correctly localized in *grdn-1* mutants. The DYF-19 and GASR-8 proteins remain localized to the ciliary base in adult wild-type animals (Mohan et al., 2013; Wei et al., 2013) despite degeneration or remodeling of the BBs in *C. elegans* embryos (Perkins et al., 1986). As expected, in wild-type animals BB fusion proteins localized to two puncta at the cilia base in AWB and one punctum in AWC (Figures 3A and 3B; Table 1). These proteins as well as the IFT-A component DAF-10, which is normally found at the BB and in the middle segment of the axoneme in AWB (Williams et al., 2011), were mislocalized to ectopic puncta or were distributed uniformly throughout the dendrites in a small but significant number of

Table 1. Girdin Regulates Localization of a Subset of TZ and BB Proteins

Strain	Cell[a]	Fusion Protein	% Cells Exhibiting Phenotype			n	p Value[b]
			At Cilia Base Only	Mislocalized	Absent		
BB Components							
Wild-Type	AWB	GFP::GASR-8	95	0	5	59	
grdn-1 (*ns303*)	AWB	GFP::GASR-8	84	14[c]	3	74	<0.05
Wild-Type	AWB	DYF-19::GFP	98	0	2	60	
grdn-1 (*ns303*)	AWB	DYF-19::GFP	75	24[d]	1	75	<0.001
Wild-Type	AWB	DAF-10::GFP	100	0	0	33	
grdn-1 (*ns303*)	AWB	DAF-10::GFP	69	21[c]	10	39	<0.001
Wild-Type	AWC	GFP::GASR-8	100	0	0	38	
grdn-1 (*ns303*)	AWC	GFP::GASR-8	44	49[e]	7	43	<0.001
grdn-1 (*hmn1*)	AWC	GFP::GASR-8	61	22[e]	17	36	<0.001
TZ Components							
Wild-Type	AWB	MKSR-2::tagRFP	87	0	13	23	
grdn-1 (*ns303*)	AWB	MKSR-2::tagRFP	60	16[d]	24	25	0.06
Wild-Type	AWB	NPHP-4::GFP	88	0	12	32	
grdn-1 (*ns303*)	AWB	NPHP-4::GFP	71	18[d]	11	45	<0.05
Wild-Type	AWB	MKS-5::GFP	90	0	10	52	
grdn-1 (*ns303*)	AWB	MKS-5::GFP	70	18[d]	12	33	<0.01
grdn-1 (*hmn1*)	AWB	MKS-5::GFP	67	28[d]	5	42	<0.001
Wild-Type	AWB	JBTS-14::GFP	86	5	9	42	
grdn-1 (*hmn1*)	AWB	JBTS-14::GFP	55	21[d]	24	38	<0.01
Wild-Type	AWC	NPHP-1::tagRFP	95	3	3	38	
grdn-1 (*ns303*)	AWC	NPHP-1::tagRFP	71	21[d]	7	14	<0.05
grdn-1 (*hmn1*)	AWC	NPHP-1::tagRFP	58	30[d]	12	43	<0.001
Wild-Type	AWC	MKSR-2::tagRFP	60	0	40	30	
grdn-1 (*hmn1*)	AWC	MKSR-2::tagRFP	34	3[d]	63	32	0.07
Wild-Type	AWC	MKS-5::tagRFP	100	0	0	40	
grdn-1 (*ns303*)	AWC	MKS-5::tagRFP	65	3[d]	32	66	<0.001
grdn-1 (*hmn1*)	AWC	MKS-5::tagRFP	65	4[d]	30	23	<0.001

Adult animals grown at 20°C were examined.
[a]AWB and AWC neurons were visualized via expression of *str-1*p::*mCherry*/*gfp* and *ceh-36*p::*gfp* (or *odr-1*p::*rfp*), respectively.
[b]Compared with wild-type within each neuron type.
[c]Fusion proteins were present at the cilia base and also mislocalized to ectopic puncta in dendrites, but not within cilia.
[d]Fusion proteins were present at the cilia base but also in ectopic puncta in dendrites, cilia, or both.
[e]Fusion proteins were present at the cilia base and also mislocalized to ectopic puncta or distributed diffusely in dendrites.

AWB and AWC neurons in *grdn-1* hypomorphic mutants (Figures 3A and 3B; Table 1). Ninety percent of neurons with mislocalized GFP::GASR-8 puncta in AWB exhibited shortened dendrites and/or cilia defects (n = 10; $p < 0.05$ compared with by chance alone), suggesting that correct GASR-8 localization to the cilia base is necessary for correct cilia and dendrite morphogenesis. Expression of these fusion proteins was also lost in a subset of animals, presumably due to degradation of mislocalized proteins (Table 1). These observations suggest that GRDN-1 regulates the localization of multiple BB components to the base of sensory cilia.

Since BBs template the TZ, we next assessed localization of TZ components in *grdn-1* mutants. While GFP-tagged MKS-5, MKSR-2, NPHP-1, NPHP-4, and JBTS-14 proteins localized to the TZs in AWB or AWC cilia in wild-type animals (Figure 3C and Table 1), these proteins were found in ectopic locations within the dendrite and occasionally within the cilium in both neuron types in *grdn-1* mutants (Figure 3C and Table 1). Since MKS-5 is essential for localizing components of the MKS/MKSR and NPHP modules (Williams et al., 2011) and is mislocalized in *grdn-1* mutants, we investigated whether multiple TZ proteins are coordinately mislocalized to ectopic puncta upon reduction of *grdn-1* function. Indeed, when mislocalized, any two TZ proteins were detected in the same ectopic locations in the majority of cells (Figure 3D). Similarly, ectopic BB and TZ protein puncta were co-localized in *grdn-1* mutants (Figure 3D). Thus, in *grdn-1* mutants, BB/TZ complexes are either assembled at ectopic locations or mislocalized following assembly at the cilia base.

To verify the presence of ectopic TZs in *grdn-1* mutants, we examined serial sections of amphid channel neurons using transmission electron microscopy (TEM). In wild-type worms,

each bilateral amphid channel pore in the nose consists of ten ciliary axonemes, arising from the dendritic endings of eight neurons (Figure S3) (Perkins et al., 1986). However, in *grdn-1* hypomorphic mutants, at least two axonemes were absent from the middle and distal regions of the pore (six pores analyzed), indicating that a subset of cilia is truncated or missing entirely (Figure S3). In addition, *grdn-1* mutants, but not wild-type animals, displayed occasional mispositioned TZs, located 5–10 μm proximal to the amphid pore (1–2 per sectioned animal) (Figure 3E). These TZs were either undocked from the dendritic plasma membrane, which extended anteriorly to the nose region, or were docked to the distal tip of a shortened dendrite (Figure 3E). Of the TZs analyzed, undocked TZs lacked an obvious cilium extension, whereas normally docked TZs at the distal ends of truncated dendrites extended a mispositioned cilium (Figure 3E). These TEM findings confirm that assembled TZs are mislocalized in *grdn-1* mutants.

Since the TZ acts as a ciliary gate regulating protein entry into and exit from the cilium (Czarnecki and Shah, 2012; Reiter et al., 2012), we tested whether ciliary proteins are also mislocalized in *grdn-1* mutants. In a subset of *grdn-1* mutants, the ciliary membrane-restricted STR-163 G-protein-coupled receptor and membrane-associated ARL-13 small guanosine triphosphatase were also found in the distal AWB dendrites (Figure S4). Conversely, the RPI-2::GFP fusion protein that is normally enriched at the dendritic tips and excluded from cilia in wild-type AWB neurons (Williams et al., 2011) was localized within AWB cilia with occasional accumulation at the distal ciliary tips in a subset of *grdn-1* mutants (Figure S4). Together, these results indicate that TZ integrity and function as a ciliary gate are partially compromised in *grdn-1* mutants.

Localization of the Cell Junction Molecule AJM-1 Is Disrupted in *grdn-1* Mutants

To further explore mechanisms of GRDN-1-mediated BB positioning and ciliogenesis, we tested pathways known to interact with Girdin in other cellular contexts. Studies in *Drosophila* and mammalian cells have implicated Girdin in cadherin-mediated cell adhesion (Houssin et al., 2015; Ichimiya et al., 2015; Muramatsu et al., 2015). Analysis of cadherin/*hmr-1* or β-catenin/*hmp-2* hypomorphs showed no defects in AWB cilia and dendrite morphology or GRDN-1 localization (Figures S5A and S5B). Moreover, AWB defects were not significantly enhanced in *hmr-1*; *grdn-1* or *hmp-2*; *grdn-1* double mutants compared with those of *grdn-1* single mutants (Figure S5A). Cadherins have been reported to function redundantly with L1CAMs to regulate cell adhesion during *C. elegans* gastrulation (Grana et al., 2010). Neither *sax-7*/LICAM single nor *hmr-1*; *sax-7* double mutants displayed AWB defects similar to those of *grdn-1* mutants (Figure S5A). These results suggest that GRDN-1 is unlikely to regulate ciliogenesis via cadherins/catenins or L1CAM in *C. elegans*.

Ultrastructural analyses have reported cell adhesion complexes—apical junctions—in distal dendritic regions of adult *C. elegans* amphid sensory neurons (Doroquez et al., 2014; Perkins et al., 1986). Indeed, AJM-1::CFP apical junction and the DYF-19::RFP BB fusion proteins localized to adjacent zones in the head when expressed in ciliated sensory neurons (Figure S5C). While localization of the AJM-1::CFP fusion protein was restricted to a narrow band in the distal AWC dendrite, this fusion protein was localized in a diffuse pattern in 30% of *grdn-1*(*ns303*) AWC dendrites (Figures 4A and 4B), implying that GRDN-1 may function at least in part via AJM-1 to mediate BB positioning and dendrite anchoring in these cells. Notably, ~80% of AWC neurons with diffuse AJM-1::CFP signal exhibited cilia or dendrite defects, and conversely, 71% of AWC neurons with morphological defects exhibited mislocalized AJM-1::CFP, suggesting that mechanisms in addition to Girdin-mediated localization of AJM-1 regulate BB positioning.

GRDN-1 Acts via CHE-10/Rootletin to Regulate Cilia Morphology in *C. elegans*

To further define mechanisms of Girdin-mediated ciliogenesis, we examined localization of proteins known to anchor BBs to the cytoskeleton in *grdn-1* mutants. Rootletin is a component of the intercentriolar linker as well as rootlets that project from the proximal centriolar regions into the cytoplasm (Yang et al., 2005, 2006). Rootlets play structural roles by tethering the BB to the actin cytoskeleton (Wolfrum, 1992; Yang et al., 2005). Rootletin has also been implicated in ciliogenesis (Conroy et al., 2012). *C. elegans* CHE-10/rootletin homolog is localized to BBs and the proximal regions of TZs in sensory cilia and is critical for maintaining the integrity of these ciliary compartments (Mohan et al., 2013). We asked whether Girdin acts via CHE-10 to regulate ciliogenesis.

CHE-10::GFP localization at the ciliary base was disrupted in *grdn-1*(*ns303*) mutants (Figures 4C and 4D). Whereas in wild-type animals CHE-10::GFP was enriched in puncta in a relatively tight zone ~11 μm from the nose tip, this fusion protein was distributed more broadly within dendrites and cilia in *grdn-1*(*ns303*) mutants (Figures 4C and 4D) (Mohan et al., 2013). Although we could not examine localization of CHE-10::GFP in *grdn-1*(*tm6493*) mutants due to their embryonic lethality, similar to our observations in the context of ciliogenesis (Figure 2E), *grdn-1*(*tm6493*) animals expressing GRDN-1(ΔCt) exhibited significant CHE-10 localization defects compared with those expressing full-length GRDN-1 (Figure 4D). In contrast, a GRDN-1a::GFP fusion protein localized normally at the AWB cilia base in *che-10*(*e1809*) larvae (Figure S5D).

Mislocalization of CHE-10 in *grdn-1* mutants could be a secondary consequence of mispositioned BBs. Alternatively, CHE-10 localization to BBs may be affected. Since it was technically challenging to assess co-localization of BBs and CHE-10 in amphid neurons, we examined CHE-10 localization relative to BBs labeled with DYF-19::eBFP in phasmid neurons. 0% and 26% of PHA/PHB phasmid neurons exhibited mislocalized BBs in wild-type and *grdn-1*(*ns303*) mutants, respectively (Figure 4E). Ninety-seven percent of BBs in wild-type animals and 91% of neurons with correctly positioned BBs in *grdn-1* mutants were associated with CHE-10 (Figure 4E). However, only 12% of neurons with mislocalized BBs exhibited CHE-10 enrichment at the BBs (Figure 4E). These data suggest that GRDN-1 regulates localization of rootletin to the BBs in *C. elegans* neurons, and that altered CHE-10 localization may underlie BB positioning defects in *grdn-1* mutants.

Cilia of amphid neurons progressively degenerate in *che-10*(*e1809*) null mutants with concomitant defects in IFT and disintegration of BB and TZ architecture that are evident largely

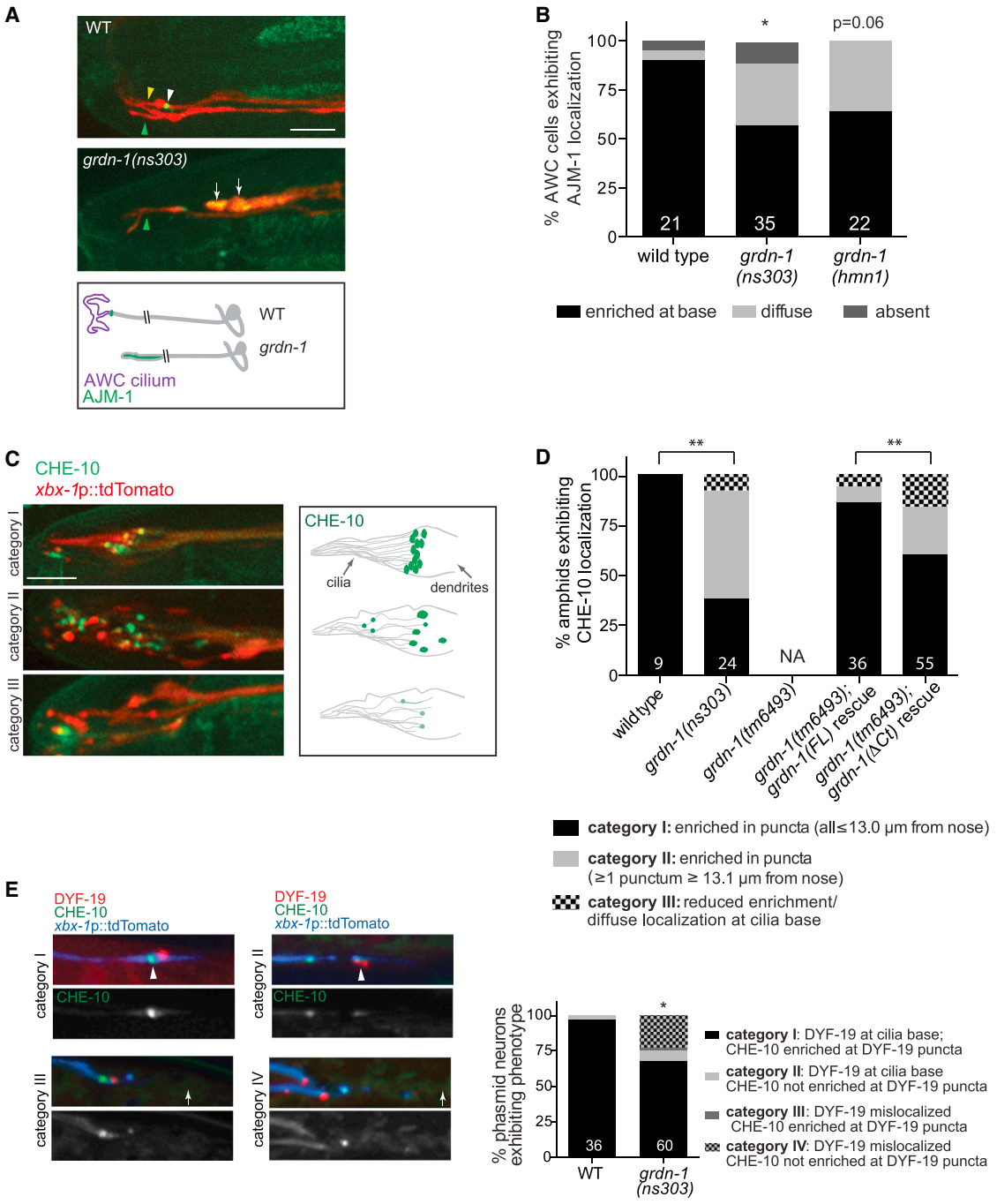

Figure 4. GRDN-1 Regulates Localization of AJM-1 and CHE-10/rootletin in *C. elegans* Sensory Neurons

(A) Images (top) and a cartoon (bottom) of AJM-1::CFP localization in AWC neurons in wild-type (WT) and *grdn-1* animals. Neurons were visualized via expression of *odr-1*p::*dsRed* in AWC and AWB. AWC is marked with yellow arrowhead (top) or drawn in purple (bottom). White arrowhead indicates the cilia base; ectopic localization is indicated by white arrows; green arrowhead marks AWB. Scale bar, 5 µm. Anterior is to the left.

(B) Quantification of AJM-1::CFP localization in AWC in wild-type and *grdn-1* mutant animals. Number of examined neurons per genotype is indicated. *$p < 0.05$, different from wild-type (Fisher's exact test).

(C) Images (left) and cartoon (right) of CHE-10::GFP localization in head ciliated neurons of wild-type and *grdn-1* animals. Scale bar, 5 µm. Anterior is to the left.

(D) Quantification of CHE-10::GFP localization in animals of the indicated genotypes. **$p < 0.01$, different between indicated values (Fisher's exact test). NA, not applicable.

(E) Images (left) and quantification (right) of CHE-10::GFP localization relative to DYF-19::eBFP puncta in adult phasmid neurons of wild-type and *grdn-1*(*ns303*) adult animals. White arrowheads mark the cilia base; white arrows mark the position where phasmid cilia normally terminate. Number of examined neurons per genotype is indicated. *$p < 0.05$, different from DYF-19/CHE-10 association predicted by chance (chi-square test). Anterior is to the left.

See also Figure S5.

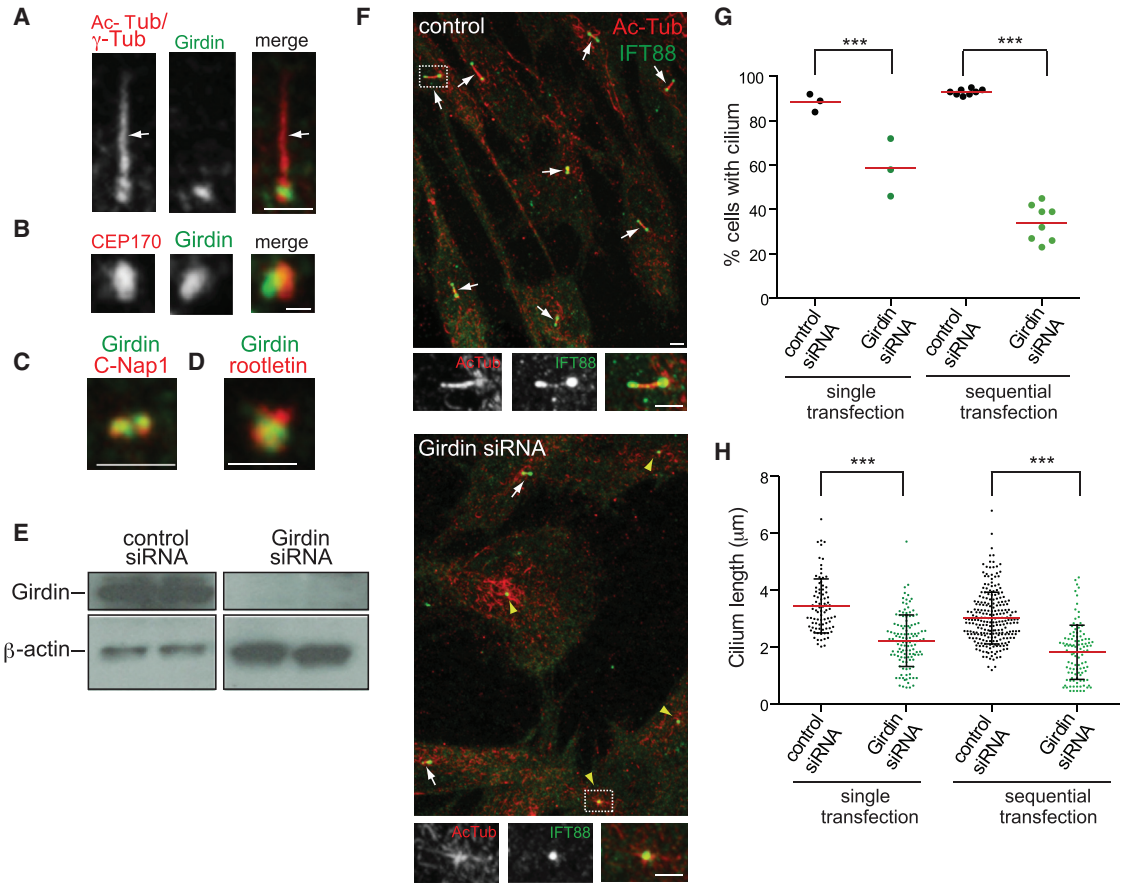

Figure 5. hGirdin Is Localized to Centrioles and Regulates Ciliogenesis in hTERT RPE-1 Cells

(A–D) Immunofluorescence images of fixed RPE-1 cells co-labeled with antibodies against the indicated proteins. The cilium is marked with white arrow in (A). Scale bars represent 2 μm in (A, C, D) and 1 μm in (B).

(E) Immunoblot of Girdin protein levels in RPE-1 cells 5 days following transfection with control or Girdin siRNA. β-Actin was used as the loading control.

(F) Images of RPE-1 cells co-stained with antibodies against AcTub and IFT88. White arrows mark cilia; yellow arrowheads mark BB-localized IFT88 in the absence of a ciliary axoneme. Boxed areas are shown at higher magnification below. Scale bars, 2 μm.

(G) Quantification of ciliation in RPE-1 cells after a single or two consecutive transfection(s) with the indicated siRNAs. Each data point represents an independent experiment; n > 140 cells per experiment per treatment. Means are indicated by horizontal red lines. ***$p < 0.001$, different between indicated values (chi-square test with Yates' correction).

(H) Quantification of cilia length in RPE-1 cells treated with control or Girdin siRNAs in single or sequential transfection experiments. Each data point represents a measurement from a single cell; n > 80 cells per treatment. Means ± SD are indicated by horizontal red bars and vertical black bars. ***$p < 0.001$, different between indicated values (Mann-Whitney test).

See also Figure S6.

in late larval stages (Mohan et al., 2013). We found that although cilia and dendrite defects were already detectable in newly hatched *grdn-1*(*ns303*) L1 animals, these defects were enhanced in adults particularly in the ASI neurons (Table S1). Thus, Girdin may play a role in both the formation and maintenance of cilia.

Girdin Is Localized to Proximal Domains of Centrioles and Regulates Ciliogenesis in Human RPE-1 Cells

We next explored whether mammalian Girdin regulates ciliogenesis. Girdin has previously been reported to be present at the centrosome in cultured cells (Ghosh et al., 2008; Mao et al., 2012). We first examined Girdin subcellular localization in RPE-1 cells that robustly ciliate upon serum starvation. Co-labeling experiments in quiescent RPE-1 cells showed that Girdin was present at the cilia base in a region that appeared to partially overlap with both centrioles (Figure 5A). Girdin localization partly overlapped with that of CEP170 (Guarguaglini et al., 2005), a marker of subdistal appendages of the mother centriole/BB (Figure 5B), but overlapped nearly completely with that of C-Nap1/CEP250, a protein present at the proximal ends of both centrioles (Fry et al., 1998) (Figure 5C). C-Nap1 directly interacts and partially co-localizes with rootletin (Yang et al., 2005, 2006). Similarly, Girdin partly co-localized with rootletin (Figure 5D).

To test whether Girdin regulates ciliogenesis in RPE-1 cells, we knocked down (knockdown: KD) Girdin with a pool of short interfering RNAs (siRNAs). Girdin KD efficiency was confirmed by western blotting of cell lysates (Figure 5E). Staining cells for AcTub or Arl13b showed reduced ciliation in Girdin compared with control siRNA-treated cells (Figures 5F and 5G). Moreover, in Girdin KD cells that retained cilia, cilium length

was significantly decreased (Figures 5F and 5H). Importantly, cells treated with single siRNAs targeting distinct non-overlapping regions of the Girdin coding sequence resulted in similar ciliogenesis defects, suggesting that the observed phenotypes are likely Girdin dependent (Figures S6A and S6B). Approximately the same fraction of control and Girdin KD cells were labeled with the proliferation marker anti-Ki67 (percentage of Ki67-positive cells: control 3%, N = 2 experiments, n > 1,000 cells; Girdin siRNA 8%, N = 3 experiments, n > 2000 cells), indicating that ciliogenesis defects in Girdin-depleted cells are not due to defects in cell-cycle exit upon serum starvation (Mao et al., 2012). Thus, as in *C. elegans*, Girdin regulates ciliogenesis in human cells.

Girdin Regulates Basal Body Position in RPE-1 Cells

Given the altered localization of BB components in *C. elegans* neurons, we examined Girdin KD cells for defects in BB position. In control RPE-1 cells, BBs labeled with anti-CEP164 are located in the cell center, near the nucleus (on average ~2 μm from the nucleus) (Figures 6A). However, Girdin KD with either a pool or two independent siRNAs increased variability in the BB-to-nucleus distance, with a fraction of BBs located at >4.0 μm from the nucleus in Girdin KD cells (Figures 6A, S6C, and S6D). Moreover, we noted a weak but significant negative correlation between cilium length and BB-to-nucleus distance upon Girdin KD (Figure 6B). Thus, as in *grdn-1* mutants, Girdin regulates BB position in human cells.

Girdin localizes to the Golgi (Le-Niculescu et al., 2005), and altered BB localization has been associated with disorganization of the Golgi network (Goncalves et al., 2010). However, staining for Golgin-97 showed no gross defects in Golgi organization or morphology in Girdin KD compared with control cells (Figure S6E), suggesting that BB mispositioning in RPE-1 cells is not a consequence of a disorganized Golgi apparatus.

BB/TZ proteins are co-recruited to mislocalized BBs in *C. elegans* (Figure 3D). We asked whether BB and TZ components are similarly recruited correctly to mislocalized BBs upon Girdin KD in RPE-1 cells. We found no obvious defects in the localization of the distal and subdistal BB appendage markers CEP164 and CEP170, respectively, or in recruitment of the IFT-B complex component IFT88 to the BB in Girdin KD cells (Figures 5F and S6E). These ciliary proteins were recruited even in cells lacking a visible ciliary axoneme (Figures 5F and S6E), indicating that Girdin is dispensable for BB maturation. Similarly, the localization of the centrosomal and TZ component CEP290 and the ciliary membrane-associated protein Arl13b were unaffected upon Girdin KD (Figures 6C and S6E). Thus, Girdin is not required for assembly of BB/TZ complexes but is required for their subcellular localization.

Girdin Regulates Rootletin Levels at the Centrioles in RPE-1 Cells

The complete and partial co-localization of Girdin with C-Nap1 and rootletin, respectively, at the proximal ends of centrioles prompted us to explore whether these proteins are interdependent for localization to the centrosome. C-Nap1 interacts with Girdin in mass spectrometry studies (Fogeron et al., 2013) and regulates rootletin localization to the centrosome (Bahe et al., 2005). Consistent with previous observations (Panic et al., 2015), we noted an increase in the percentage of cells with split centrioles upon C-Nap1 KD, confirming efficient KD of this protein (0% and 37% of centrioles were located at distances >2.0 μm from each other in control and C-Nap1 KD RPE-1 cells, respectively; n ≥ 50 cells each). C-Nap1 KD significantly reduced Girdin centriolar signal levels (Figure 6D), suggesting that C-Nap1 regulates Girdin localization to the proximal ends of centrioles.

We next tested whether, as in *C. elegans*, Girdin functions in part via rootletin to regulate BB localization and ciliogenesis in RPE-1 cells. Indeed Girdin KD RPE-1 cells displayed reduced rootletin levels at the BB (Figure 6E). Rootletin siRNA treatment markedly reduced rootletin levels at the centrosome (Figure 6F), confirming KD efficiency, and, moreover, disrupted BB localization relative to the nucleus and impaired ciliogenesis (Figures 6F and 6G). The latter phenotypes resembled those observed upon Girdin KD. Although rootletin depletion has also been shown to induce centriole splitting (Bahe et al., 2005; Conroy et al., 2012; Yang et al., 2006), we did not observe centriole splitting by anti-γ-tubulin or anti-Centrin-2 immunostaining upon Girdin or rootletin KD in RPE-1 cells (<6% of centrioles were located >2.0 μm from each other in Girdin KD, rootletin KD, or control cells; n > 50 cells each [Figure S6D]). However, we cannot exclude the possibility that centriole tethering is partially affected upon Girdin and rootletin KD. Together, these observations suggest that Girdin regulates BB localization and ciliogenesis, in part via rootletin, in both *C. elegans* and human cells (Figure 6H).

DISCUSSION

Girdin Positions Basal Bodies in Ciliated Cells

Our results indicate that Girdin is required to correctly position BBs to regulate ciliogenesis in *C. elegans* sensory neurons and RPE-1 cells. This conclusion is based on three experimental observations. First, in both systems Girdin is localized to the proximal domains of BBs. In *C. elegans* sensory neurons, Girdin expression overlaps with the developmental window during which the core BB proteins are present at the cilia base. Moreover, the temporal requirement for Girdin function in ciliogenesis coincides with the time period of birth and differentiation of sensory neurons (Dammermann et al., 2009; Sulston et al., 1983). Second, BBs are mislocalized upon reduction of Girdin function in both nematode sensory neurons and in RPE-1 cells. Third, reduction of Girdin function impairs ciliogenesis in multiple sensory neuron types in *C. elegans* as well as in RPE-1 cells. In addition, mislocalization of BB proteins in *grdn-1* mutants in *C. elegans* and an increase in BB-to-nucleus distance in RPE-1 cells are correlated with cilia morphology defects. This remarkable conservation of Girdin function in *C. elegans* and human cells highlights the critical contribution of Girdin to BB localization and cilia formation.

Girdin Acts via Multiple Pathways to Position BBs in *C. elegans* Amphid Sensory Neurons

Girdin is required for correct localization of CHE-10/rootletin at the ciliary base in *C. elegans* ciliated sensory neurons. In addition to being a major component of the intercentriolar linker, rootletin is a constituent of ciliary rootlet fibers that originate from the proximal ends of BBs in ciliated cells including a subset of

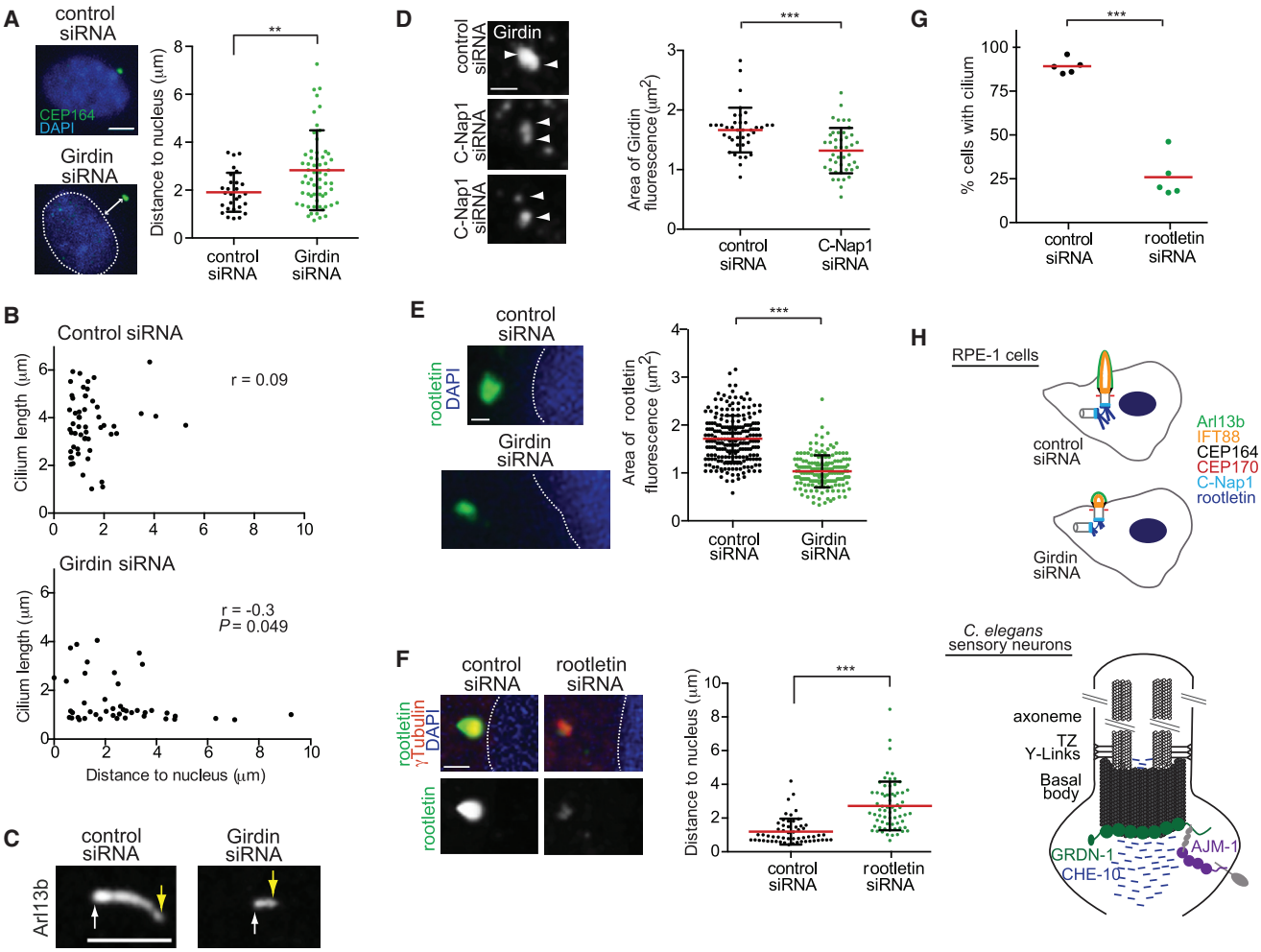

Figure 6. Girdin Regulates BB Position and Rootletin Levels at Centrioles in RPE-1 Cells

(A) (Left) Images of RPE-1 cells sequentially treated with control or Girdin siRNAs, serum starved for 48 hr, and stained for anti-CEP164 and DAPI to mark BBs and nuclei, respectively. White double headed arrow marks BB-to-nucleus distance quantified in the scatterplot (right). Each data point represents a value from a single cell; n > 25 cells per treatment; at least two independent experiments. Means ± SD are indicated by horizontal red bars and vertical black bars. **p < 0.01, different between indicated values (Mann-Whitney test). Scale bar, 2 μm. White dashed line outlines the nucleus.

(B) Correlation between ciliary length and BB-to-nucleus distance in control and Girdin siRNA-treated cells. r, Pearson correlation coefficient.

(C) Images of RPE-1 cells sequentially treated with control or Girdin siRNAs, serum starved for 48 hr, and stained for Arl13b. White arrows mark the ciliary base; yellow arrows mark the ciliary tip. Scale bar, 5 μm.

(D) (Left) Images of RPE-1 cells treated with control or C-Nap1/CEP250 siRNAs, serum starved for 48 hr, and labeled with anti-Girdin. White arrowheads mark centrioles. Scale bar, 2 μm. (Right) Quantification of Girdin localization in control and C-Nap1 siRNA-treated cells. Each data point represents a value from a single cell; n > 30 cells per treatment; at least three independent experiments. Means ± SD are indicated by horizontal red bars and vertical black bars. ***p < 0.001, different between indicated values (Mann-Whitney test).

(E) (Left) Images of RPE-1 cells sequentially treated with control or Girdin siRNAs, serum starved for 48 hr, and stained with anti-rootletin and DAPI. White dashed lines outline the nuclei. Scale bar, 1 μm. (Right) Quantification of rootletin area of fluorescence in control and Girdin siRNA-treated cells. Each dot represents a value from a single cell; n > 160 cells per treatment; at least three independent experiments. Means ± SD are indicated by horizontal red bars and vertical black bars. ***p < 0.001, different between indicated values (Mann-Whitney test).

(F) (Left) Images of control or rootletin siRNA-treated RPE-1 cells stained with DAPI and antibodies against γ-tubulin and rootletin. (Right) Scatterplot quantifying BB-to-nucleus distance in control and rootletin siRNA-treated cells. Each data point represents a value from a single cell; n > 50 cells per treatment; at least three independent experiments. Means ± SD are indicated by horizontal red bars and vertical black bars. ***p < 0.001, different between indicated values (Mann-Whitney test). Scale bar, 2 μm. White dashed lines mark nuclear boundaries.

(G) Quantification of ciliation in RPE-1 cells after two consecutive transfections with control or rootletin siRNAs. Each data point represents an independent experiment; n > 100 cells per experiment per treatment. Means are indicated by horizontal red lines. ***p < 0.001, different between indicated values (Fisher's exact test).

(H) (Top) Schematic summarizing effects of Girdin depletion on the localization of centrosomal and ciliary proteins in RPE-1 cells. (Bottom) Cartoon of GRDN-1-mediated BB positioning mechanisms in *C. elegans* ciliated sensory neurons. As yet unidentified components at the ciliary base are indicated in gray.

non-amphid *C. elegans* sensory neurons (Mohan et al., 2013; Yang et al., 2002). Although amphid sensory neurons in *C. elegans* do not contain obvious rootlets, electron-dense rootlet-like structures have been noted in close proximity to the cilia base in these neurons (Doroquez et al., 2014; Perkins et al., 1986). In *che-10* mutants, these cilia undergo progressive degeneration accompanied by loss of BB/TZ proteins (Mohan et al., 2013). Thus, these rootlet-like complexes may have a structural role in maintaining ciliary integrity in these sensory neurons. We propose that altered BB localization upon reduction of Girdin function results in part from disruption of CHE-10/rootletin-mediated anchoring of BBs to the cellular cytoskeleton. This hypothesis is further supported by our observation that the C-terminal domain of GRDN-1 is essential for both ciliogenesis and regulation of CHE-10 localization.

GRDN-1 may also act via additional mechanisms to regulate BB localization. BBs in *C. elegans* amphid neurons are located at the distal dendritic tips, and apical junctions have been detected in these regions by electron microscopy (Doroquez et al., 2014; Perkins et al., 1986). We find that AJM-1 localizes to distal dendritic regions adjacent to BBs and that AJM-1 localization is disrupted in *grdn-1* mutants. Based on these findings, we suggest that GRDN-1 regulates BB positioning in *C. elegans* sensory dendrites via at least two molecular pathways: AJM-1-mediated anchoring to the plasma membrane, and rootletin-dependent anchoring to the cytoskeleton. However, we are unable to exclude the possibility that GRDN-1 also acts via as yet unidentified pathways to regulate one or more of these processes. In the future, it will be important to identify additional components of the GRDN-1/CHE-10/AJM-1 complex, and examine the mechanistic hierarchy that governs correct BB localization.

Girdin Localizes BBs via Partly Conserved Mechanisms

The mechanism by which Girdin regulates BB positioning is partly conserved between *C. elegans* and human cells. As in *C. elegans*, Girdin localizes to the proximal regions of centrioles in ciliated RPE-1 cells. We find that Girdin levels at the BB are regulated by C-Nap1, and that Girdin, in turn, regulates rootletin levels at the BB in RPE-1 cells. Thus, Girdin may mediate rootletin recruitment to the centrioles either downstream of, and/or in parallel with, C-Nap1 to position BBs and control ciliogenesis in mammalian cells. Consistent with this hypothesis, similar to Girdin depletion, reduction of rootletin levels leads to defects in ciliogenesis and BB positioning. Recent work has demonstrated that MTs and intercentriolar linker proteins coordinately regulate centrosome cohesion and positioning in RPE-1 cells (Panic et al., 2015). Although the N-terminal Hook domain of Girdin does not appear to be required for ciliogenesis in *C. elegans*, this domain may directly interact with MTs to contribute to BB positioning in mammalian cells.

Is Girdin function conserved in *Drosophila*? A recent study has shown that ciliated sensory neuron dendrites in *Drosophila* Girdin (dGirdin) mutants exhibit a progressive degeneration phenotype, possibly due to a lack of dGirdin-mediated stabilization of their dendritic tips (Ha et al., 2015). Although cilia formation appears to be defective in these mutants, it is currently unclear whether these defects are secondary to their dendritic morphogenesis defects. dGirdin exhibits a complex localization pattern with possible association with BBs (Ha et al., 2015). However, it is unknown whether BBs are mislocalized in dGirdin mutants. Intriguingly, a small percentage of *grdn-1* mutants also exhibits variably shortened and/or branched amphid sensory neuron dendrites in *C. elegans*. It has been previously noted that TZ mutants also display similar dendritic morphology defects (Schouteden et al., 2015; Williams et al., 2011), suggesting that Girdin and the TZ complex may coordinately anchor the distal dendritic tips in *C. elegans*. Thus, the role of Girdin in regulating aspects of ciliated neuron morphology may also be conserved between *C. elegans* and *Drosophila*.

Concluding Remarks

A role for Girdin in regulating BB localization and ciliogenesis has intriguing implications for our understanding of the function of this protein in other cellular processes. For instance, Girdin regulates the migration of both neuronal and non-neuronal cells in normal and malignant contexts (Enomoto et al., 2005; Weng et al., 2010). The positioning of the centrosome relative to the nucleus has been suggested to be important in regulating polarity in migrating cells (Elric and Etienne-Manneville, 2014; Luxton and Gundersen, 2011), and the position and orientation of cilia contribute to the correct trajectory of migration of neurons and fibroblasts (Baudoin et al., 2012; Higginbotham et al., 2012; Schneider et al., 2010). These observations raise the possibility that altered ciliogenesis and centrosome positioning may in part underlie Girdin-dependent phenotypes in the above cellular contexts. Given the proposed role for Girdin as a signaling and scaffolding hub, a major goal for the future will be to dissect the multiple roles of Girdin and determine their contributions to specific cellular pathways.

EXPERIMENTAL PROCEDURES

C. elegans Genetics

At least two independent lines were examined for each extrachromosomal array, and data from one representative line were reported. For the experiments carried out in the *grdn-1*(*tm6493*) background, data from one or two representative lines were reported. When applicable, extrachromosomal arrays in wild-type animals were crossed into the relevant mutant strains such that expression from the same arrays was compared across strains. The complete list of strains used in this work is provided in Table S2.

Molecular Biology

DNA constructs used to generate transgenic strains are described in detail in Supplemental Experimental Procedures.

Cell Culture and Transfection

Human telomerase-immortalized retinal pigment epithelial cells (hTERT RPE-1, a gift of H. Khanna, University of Massachusetts Medical School) were cultured in DMEM/F-12 (1:1) supplemented with 10% fetal bovine serum and 1× antibiotic-antimycotic (Life Technologies). Human ON-TARGETplus Girdin (pools and single siRNA oligonucleotides), rootletin, and C-Nap1 siRNAs and non-targeting siRNA #1 were purchased from Dharmacon. Cells were serum starved for either 48 or 96 hr to induce ciliation. C-Nap1 and rootletin KD was verified by immunofluorescence and/or phenotypic analysis. For sequential transfection, two consecutive siRNA transfections were performed at a 48-hr interval.

Immunostaining

RPE-1 cells were fixed with ice-cold methanol at −20°C for 7 min, ice-cold acetone at −20°C for 3 min, or 10% formalin solution at room temperature for 12 min followed by three brief washes in PBS or PBST (PBS and 0.1% Triton

X-100, following formalin fixation only). Fixed cells were blocked with 5% BSA in PBS for 10 min followed by incubation in primary antibodies for 1 hr at room temperature or overnight at 4°C. Species-specific fluorophore-conjugated secondary antibodies were applied for 1 hr at room temperature. Antibodies used for immunostaining and immunoblotting are listed in Supplemental Experimental Procedures.

Microscopy

For visualization and quantification of cilia morphologies in *C. elegans*, animals were imaged on an inverted spinning-disk confocal microscope (Zeiss Axiovert with a Yokogawa CSU22 spinning-disk confocal head). Fixed and stained RPE-1 cells were imaged on an upright Imager.M2 (Zeiss) microscope or on an inverted spinning-disk confocal microscope. For TEM, 1-day-old adult worms were fixed overnight at 4°C in 2.5% glutaraldehyde (+1% paraformaldehyde in Sørensen's buffer), and sectioned and imaged as described previously (Sanders et al., 2015).

Statistical Analysis

Prism6 (GraphPad software) was used to perform statistical analysis and generate bar graphs and scatterplots in all figures.

SUPPLEMENTAL INFORMATION

Supplemental Information includes Supplemental Experimental Procedures, six figures, and two tables and can be found with this article online at http://dx.doi.org/10.1016/j.devcel.2016.07.013.

AUTHOR CONTRIBUTIONS

Conceptualization: I.V.N., A.O.-M., and P.S.; Methodology: I.V.N. and A.O-M.; Investigation – Genetics, Molecular Biology, Microscopy, Cell Culture: I.V.N., A.O-M., and A.K.; Investigation – TEM: J.K. and O.E.B.; Resources: I.G.M. and M.G.H.; Writing: I.V.N. and P.S.; Supervision and Funding Acquisition: P.S.

ACKNOWLEDGMENTS

We thank S. Shaham for sharing unpublished data and reagents, M. Leroux, M. Barr, J. Hu, and H. Khanna for reagents, and the CGC and NBRP (Japan) for strains. We are grateful to the Sengupta laboratory for discussions and critical comments on the manuscript. This work was supported in part by the NIH (R37 GM56223 to P.S.; F31 DC010090 to A.O.-M.), a March of Dimes Basil O'Connor Starter Scholar Research Award (5-FY11-574 to M.G.H.), an NSF Graduate Research Fellowship (to I.G.M.), a Science Foundation Ireland Principal Investigator Award (SF1-11-1037 to O.E.B.), and the European Community's Seventh Framework Program FP7/2009 under grant agreement 241955 SYSCILIA (to O.E.B.).

Received: August 31, 2015
Revised: March 9, 2016
Accepted: July 17, 2016
Published: August 18, 2016

REFERENCES

Bacaj, T., Tevlin, M., Lu, Y., and Shaham, S. (2008). Glia are essential for sensory organ function in *C. elegans*. Science *322*, 744–747.

Bahe, S., Stierhof, Y.D., Wilkinson, C.J., Leiss, F., and Nigg, E.A. (2005). Rootletin forms centriole-associated filaments and functions in centrosome cohesion. J. Cell Biol. *171*, 27–33.

Baudoin, J.P., Viou, L., Launay, P.S., Luccardini, C., Espeso Gil, S., Kiyasova, V., Irinopoulou, T., Alvarez, C., Rio, J.P., Boudier, T., et al. (2012). Tangentially migrating neurons assemble a primary cilium that promotes their reorientation to the cortical plate. Neuron *76*, 1108–1122.

Brown, J.M., and Witman, G.B. (2014). Cilia and diseases. Bioscience *64*, 1126–1137.

Coleman, B.D., Marivin, A., Parag-Sharma, K., DiGiacomo, V., Kim, S., Pepper, J.S., Casler, J., Nguyen, L.T., Koelle, M.R., and Garcia-Marcos, M. (2016). Evolutionary conservation of a GPCR-independent mechanism of trimeric G protein activation. Mol. Biol. Evol. *33*, 820–837.

Conroy, P.C., Saladino, C., Dantas, T.J., Lalor, P., Dockery, P., and Morrison, C.G. (2012). C-NAP1 and rootletin restrain DNA damage-induced centriole splitting and facilitate ciliogenesis. Cell Cycle *11*, 3769–3778.

Czarnecki, P.G., and Shah, J.V. (2012). The ciliary transition zone: from morphology and molecules to medicine. Trends Cell Biol. *22*, 201–210.

Dammermann, A., Pemble, H., Mitchell, B.J., McLeod, I., Yates, J.R., 3rd, Kintner, C., Desai, A.B., and Oegema, K. (2009). The hydrolethalus syndrome protein HYLS-1 links core centriole structure to cilia formation. Genes Dev. *23*, 2046–2059.

Dawe, H.R., Farr, H., and Gull, K. (2007). Centriole/basal body morphogenesis and migration during ciliogenesis in animal cells. J. Cell Sci. *120*, 7–15.

Doroquez, D.B., Berciu, C., Anderson, J.R., Sengupta, P., and Nicastro, D. (2014). A high-resolution morphological and ultrastructural map of anterior sensory cilia and glia in *C. elegans*. Elife *3*, e01948.

Elric, J., and Etienne-Manneville, S. (2014). Centrosome positioning in polarized cells: common themes and variations. Exp. Cell Res. *328*, 240–248.

Enomoto, A., Murakami, H., Asai, N., Morone, N., Watanabe, T., Kawai, K., Murakumo, Y., Usukura, J., Kaibuchi, K., and Takahashi, M. (2005). Akt/PKB regulates actin organization and cell motility via Girdin/APE. Dev. Cell *9*, 389–402.

Enomoto, A., Ping, J., and Takahashi, M. (2006). Girdin, a novel actin-binding protein, and its family of proteins possess versatile functions in the Akt and Wnt signaling pathways. Ann. NY Acad. Sci. *1086*, 169–184.

Fogeron, M.L., Muller, H., Schade, S., Dreher, F., Lehmann, V., Kuhnel, A., Scholz, A.K., Kashofer, K., Zerck, A., Fauler, B., et al. (2013). LGALS3BP regulates centriole biogenesis and centrosome hypertrophy in cancer cells. Nat. Commun. *4*, 1531.

Fry, A.M., Mayor, T., Meraldi, P., Stierhof, Y.D., Tanaka, K., and Nigg, E.A. (1998). C-Nap1, a novel centrosomal coiled-coil protein and candidate substrate of the cell cycle-regulated protein kinase Nek2. J. Cell Biol. *141*, 1563–1574.

Garcia-Marcos, M., Ghosh, P., and Farquhar, M.G. (2015). GIV/Girdin transmits signals from multiple receptors by triggering trimeric G protein activation. J. Biol. Chem. *290*, 6697–6704.

Ghosh, P., Garcia-Marcos, M., Bornheimer, S.J., and Farquhar, M.G. (2008). Activation of Galphai3 triggers cell migration via regulation of GIV. J. Cell Biol. *182*, 381–393.

Goncalves, J., Nolasco, S., Nascimento, R., Lopez Fanarraga, M., Zabala, J.C., and Soares, H. (2010). TBCCD1, a new centrosomal protein, is required for centrosome and Golgi apparatus positioning. EMBO Rep. *11*, 194–200.

Grana, T.M., Cox, E.A., Lynch, A.M., and Hardin, J. (2010). SAX-7/L1CAM and HMR-1/cadherin function redundantly in blastomere compaction and non-muscle myosin accumulation during *Caenorhabditis elegans* gastrulation. Dev. Biol. *344*, 731–744.

Guarguaglini, G., Duncan, P.I., Stierhof, Y.D., Holmstrom, T., Duensing, S., and Nigg, E.A. (2005). The forkhead-associated domain protein Cep170 interacts with Polo-like kinase 1 and serves as a marker for mature centrioles. Mol. Biol. Cell *16*, 1095–1107.

Ha, A., Polyanovsky, A., and Avidor-Reiss, T. (2015). *Drosophila* hook-related protein (Girdin) is essential for sensory dendrite formation. Genetics *200*, 1149–1159.

Heiman, M.G., and Shaham, S. (2009). DEX-1 and DYF-7 establish sensory dendrite length by anchoring dendritic tips during cell migration. Cell *137*, 344–355.

Higginbotham, H., Eom, T.Y., Mariani, L.E., Bachleda, A., Hirt, J., Gukassyan, V., Cusack, C.L., Lai, C., Caspary, T., and Anton, E.S. (2012). Arl13b in primary cilia regulates the migration and placement of interneurons in the developing cerebral cortex. Dev. Cell *23*, 925–938.

Houssin, E., Tepass, U., and Laprise, P. (2015). Girdin-mediated interactions between cadherin and the actin cytoskeleton are required for epithelial morphogenesis in *Drosophila*. Development *142*, 1777–1784.

Ichimiya, H., Maeda, K., Enomoto, A., Weng, L., Takahashi, M., and Murohara, T. (2015). Girdin/GIV regulates transendothelial permeability by controlling VE-cadherin trafficking through the small GTPase, R-Ras. Biochem. Biophys. Res. Commun. *461*, 260–267.

Lancaster, M.A., and Gleeson, J.G. (2009). The primary cilium as a cellular signaling center: lessons from disease. Curr. Opin. Genet. Dev. *19*, 220–229.

Lanjuin, A., VanHoven, M.K., Bargmann, C.I., Thompson, J.K., and Sengupta, P. (2003). *Otx/otd* homeobox genes specify distinct sensory neuron identities in *C. elegans*. Dev. Cell *5*, 621–633.

Le-Niculescu, H., Niesman, I., Fischer, T., DeVries, L., and Farquhar, M.G. (2005). Identification and characterization of GIV, a novel Galpha i/s-interacting protein found on COPI, endoplasmic reticulum-Golgi transport vesicles. J. Biol. Chem. *280*, 22012–22020.

Luxton, G.W., and Gundersen, G.G. (2011). Orientation and function of the nuclear-centrosomal axis during cell migration. Curr. Opin. Cell Biol. *23*, 579–588.

Mao, J.Z., Jiang, P., Cui, S.P., Ren, Y.L., Zhao, J., Yin, X.H., Enomoto, A., Liu, H.J., Hou, L., Takahashi, M., et al. (2012). Girdin locates in centrosome and midbody and plays an important role in cell division. Cancer Sci. *103*, 1780–1787.

Mohan, S., Timbers, T.A., Kennedy, J., Blacque, O.E., and Leroux, M.R. (2013). Striated rootlet and nonfilamentous forms of rootletin maintain ciliary function. Curr. Biol. *23*, 2016–2022.

Muramatsu, A., Enomoto, A., Kato, T., Weng, L., Kuroda, K., Asai, N., Asai, M., Mii, S., and Takahashi, M. (2015). Potential involvement of kinesin-1 in the regulation of subcellular localization of Girdin. Biochem. Biophys. Res. Commun. *463*, 999–1005.

Oshita, A., Kishida, S., Kobayashi, H., Michiue, T., Asahara, T., Asashima, M., and Kikuchi, A. (2003). Identification and characterization of a novel Dvl-binding protein that suppresses Wnt signalling pathway. Genes Cells *8*, 1005–1017.

Panic, M., Hata, S., Neuner, A., and Schiebel, E. (2015). The centrosomal linker and microtubules provide dual levels of spatial coordination of centrosomes. PLoS Genet. *11*, e1005243.

Perkins, L.A., Hedgecock, E.M., Thomson, J.N., and Culotti, J.G. (1986). Mutant sensory cilia in the nematode *Caenorhabditis elegans*. Dev. Biol. *117*, 456–487.

Reiter, J.F., Blacque, O.E., and Leroux, M.R. (2012). The base of the cilium: roles for transition fibres and the transition zone in ciliary formation, maintenance and compartmentalization. EMBO Rep. *13*, 608–618.

Sanders, A.A., Kennedy, J., and Blacque, O.E. (2015). Image analysis of *Caenorhabditis elegans* ciliary transition zone structure, ultrastructure, molecular composition, and function. Methods Cell Biol. *127*, 323–347.

Schneider, L., Cammer, M., Lehman, J., Nielsen, S.K., Guerra, C.F., Veland, I.R., Stock, C., Hoffmann, E.K., Yoder, B.K., Schwab, A., et al. (2010). Directional cell migration and chemotaxis in wound healing response to PDGF-AA are coordinated by the primary cilium in fibroblasts. Cell Physiol. Biochem. *25*, 279–292.

Schouteden, C., Serwas, D., Palfy, M., and Dammermann, A. (2015). The ciliary transition zone functions in cell adhesion but is dispensable for axoneme assembly in *C. elegans*. J. Cell Biol. *210*, 35–44.

Shen, Z., Zhang, X., Chai, Y., Zhu, Z., Yi, P., Feng, G., Li, W., and Ou, G. (2014). Conditional knockouts generated by engineered CRISPR-Cas9 endonuclease reveal the roles of coronin in *C. elegans* neural development. Dev. Cell *30*, 625–636.

Starich, T.A., Herman, R.K., Kari, C.K., Yeh, W.-H., Schackwitz, W.S., Schuyler, M.W., Collet, J., Thomas, J.H., and Riddle, D.L. (1995). Mutations affecting the chemosensory neurons of *Caenorhabditis elegans*. Genetics *139*, 171–188.

Sulston, J.E., Schierenberg, E., White, J.G., and Thomson, J.N. (1983). The embryonic cell lineage of the nematode *Caenorhabditis elegans*. Dev. Biol. *100*, 64–119.

Tang, N., and Marshall, W.F. (2012). Centrosome positioning in vertebrate development. J. Cell Sci. *125*, 4951–4961.

Walton, T., Preston, E., Nair, G., Zacharias, A.L., Raj, A., and Murray, J.I. (2015). The Bicoid class homeodomain factors *ceh-36*/OTX and *unc-30*/PITX cooperate in *C. elegans* embryonic progenitor cells to regulate robust development. PLoS Genet. *11*, e1005003.

Ward, S., Thomson, N., White, J.G., and Brenner, S. (1975). Electron microscopical reconstruction of the anterior sensory anatomy of the nematode *Caenorhabditis elegans*. J. Comp. Neurol. *160*, 313–337.

Ware, R.W., Clark, D., Crossland, K., and Russell, R.L. (1975). The nerve ring of the nematode *Caenorhabditis elegans*: sensory input and motor output. J. Comp. Neurol. *162*, 71–110.

Wei, Q., Xu, Q., Zhang, Y., Li, Y., Zhang, Q., Hu, Z., Harris, P.C., Torres, V.E., Ling, K., and Hu, J. (2013). Transition fibre protein FBF1 is required for the ciliary entry of assembled intraflagellar transport complexes. Nat. Commun. *4*, 2750.

Weng, L., Enomoto, A., Ishida-Takagishi, M., Asai, N., and Takahashi, M. (2010). Girding for migratory cues: roles of the Akt substrate Girdin in cancer progression and angiogenesis. Cancer Sci. *101*, 836–842.

Williams, C.L., Li, C., Kida, K., Inglis, P.N., Mohan, S., Semenec, L., Bialas, N.J., Stupay, R.M., Chen, N., Blacque, O.E., et al. (2011). MKS and NPHP modules cooperate to establish basal body/transition zone membrane associations and ciliary gate function during ciliogenesis. J. Cell Biol. *192*, 1023–1041.

Wolfrum, U. (1992). Cytoskeletal elements in arthropod sensilla and mammalian photoreceptors. Biol. Cell *76*, 373–381.

Yang, J., Liu, X., Yue, G., Adamian, M., Bulgakov, O., and Li, T. (2002). Rootletin, a novel coiled-coil protein, is a structural component of the ciliary rootlet. J. Cell Biol. *159*, 431–440.

Yang, J., Gao, J., Adamian, M., Wen, X.H., Pawlyk, B., Zhang, L., Sanderson, M.J., Zuo, J., Makino, C.L., and Li, T. (2005). The ciliary rootlet maintains long-term stability of sensory cilia. Mol. Cell Biol. *25*, 4129–4137.

Yang, J., Adamian, M., and Li, T. (2006). Rootletin interacts with C-Nap1 and may function as a physical linker between the pair of centrioles/basal bodies in cells. Mol. Biol. Cell *17*, 1033–1040.